# Distorted-wave theory of heavy-particle collisions at intermediate energies

S. Bienstock
*Harvard-Smithsonian Center for Astrophysics, Cambridge, Massachusetts 02138*

T. G. Heil
*Department of Physics and Astronomy, University of Georgia, Athens, Georgia 30602*

A. Dalgarno
*Harvard-Smithsonian Center for Astrophysics, Cambridge, Massachusetts 02138*
(Received 25 August 1983)

The quantum-mechanical description of heavy-particle collisions is extended to the intermediate-energy range through the use of a second-order distorted-wave approximation. Cross sections are calculated using close-coupled solutions for low partial waves and first- and second-order unitarized distorted-wave solutions for higher partial waves where the distorted-wave method is accurate. The method is applied to the calculation of charge transfer cross sections for collisions of $C^{3+}$ with H, and of $O^{2+}$ with He over the energy range 0—5 keV/amu, and to investigate the influence of the charge transfer channel on ion-impact excitation of $O^+$.

## I. INTRODUCTION

Charge transfer processes of multiply charged ions in collision with neutral atomic systems affect the ionization structure and impurity transport, the thermal balance, and the radiation losses of plasmas. Heil, Butler, and Dalgarno[1] have presented a close-coupled quantum theory of low-energy charge transfer processes and applied it to calculate rate coefficients for charge transfer in collisions of neutral hydrogen atoms with doubly and triply charged ions of carbon, nitrogen, oxygen, and neon at temperatures obtaining in astrophysical nebulae, corresponding to collision energies of less than 10 eV/amu. Charge transfer reactions are important also in fusion plasmas, particularly near the plasma edge, but the relevant collision energies are above 100 eV/amu. In their calculations, Heil *et al.*[1] solved the equations of quantal close-coupling theory by numerical integration, a procedure which is impractical at high energies. We present here a unitarized, multichannel distorted-wave approximation which can be carried through readily to second order in the coupling strength and which improves rapidly in accuracy as the energy $E$ and the nuclear angular momentum quantum number $J$ increase. We have constructed a systematic procedure in which for a given energy close-coupling results are used for small values of $J$, second-order distorted-wave results are used for intermediate values of $J$, and first-order distorted-wave results are used for large values of $J$, each approximation giving way to the simpler more economical one as it becomes sufficiently accurate.

We explore the method by varying the coupling strengths for the reaction

$$C^{3+}(2s,\,^2S)+H\rightarrow C^{2+}+H^+\,, \tag{1}$$

for which we have previously reported the cross sections, and we use it to calculate cross sections for the charge transfer reaction

$$O^{2+}(2s^22p^2,\,^3P)+He\rightarrow O^+ + He^+\,. \tag{2}$$

We explore also the influence of the charge transfer channel on the ion-impact excitation process

$$He^+ + O^+(2s^22p^3,\,^2D^o)\rightarrow He^+ + O^+(2s^22p^3,\,^2P^o)\,. \tag{3}$$

## II. ADIABATIC AND DIABATIC FORMULATIONS

Heil *et al.*[1] have given a quasimolecular quantal adiabatic description of the collision of a heavy ion with a light atom, involving transitions between states of the same molecular symmetry. After selecting those adiabatic states for which the radial coupling is large at some separation, they transformed to the diabatic basis called the $P$-diabatic representation by Delos and Thorson.[2] In this basis the inelastic and the reactive processes are driven by the off-diagonal elements of a symmetric potential-energy matrix $\underline{V}(R)$, whose diagonal elements are diabatic potential-energy curves, $R$ being the nuclear separation. The scattering equations take the form

$$\left[\frac{\hbar^2}{2\mu}\nabla_R^2\underline{I}-\underline{V}(R)+E\underline{I}\right]\underline{F}(\vec{\mathrm{R}})=\underline{0}\,, \tag{4}$$

where $\underline{F}(\vec{\mathrm{R}})$ is a column matrix of scattering functions $F_i(\vec{\mathrm{R}})$, $E$ is the energy of relative motion in the entrance channel, and $\mu$ is the reduced mass. At large distances, $\underline{V}(R)$ tends to a diagonal matrix with elements $V_i$.

After expansion of $\underline{F}(\vec{\mathrm{R}})$ in total angular momentum functions, the radial functions $\underline{\chi}^J(R)$ satisfy for each $J$ the coupled differential equations

$$\left[\frac{d^2}{dR^2}\underline{I}+\underline{k}^2-\frac{J(J+1)}{R^2}\underline{I}\right]\underline{\chi}^J+\underline{U}(R)\underline{\chi}^J\,, \tag{5}$$

 

where $\underline{k}^2$ is a diagonal matrix with elements $k_i^2=2\mu(E-V_i)/\hbar^2$, $\underline{U}=2\mu\underline{V}/\hbar^2$, and we have taken the projection of the electronic angular momentum on to the internuclear axis to be zero. The total cross section $\sigma(E)$ at an energy $E$ can be written as the weighted sum

$$\sigma(E)=\sum_s w_s\sigma_s(E) , \tag{6}$$

where $\sigma_s$ is the cross section for charge transfer in the particular molecular symmetry and $w_s$ is the statistical weight $(2S+1)(2-\delta_{\Lambda,0})/\sum_s w_s$.

The cross section in each symmetry is expressed as the sum

$$\sigma_s(E)=\frac{\pi\hbar^2}{2\mu E}\sum_J\sum_j(2J+1)\,|\,S_{ij}-\delta_{ij}\,|^2 , \tag{7}$$

where $S_{ij}$ is the scattering matrix element connecting the initial state $i$ to a final state $j$ formed by charge transfer or excitation. The $S$-matrix elements are obtained from the asymptotic behavior of the radial functions, which in turn are determined by solving the coupled radial equations (5). The form of equations (5) makes them particularly amenable to numerical solution by standard techniques at low energy. With increasing energy the number of partial waves which contribute to $\sigma_s(E)$ rapidly becomes very large and a more economical procedure is needed. A semiclassical unitarized distorted-wave approximation has been developed by Ryufuku and Watanabe.[3] Because the distortion potential in the entrance channel is qualitatively different from the repulsive Coulomb potential which characterizes the asymptotic behavior of all the exit channels, and because we wished to obtain a procedure which extrapolated smoothly from low to intermediate energies, we chose to avoid the introduction of a classical description of the nuclear motion and we instead developed an algorithm based upon the quantum-mechanical distorted-wave approximation.

## III. DISTORTED-WAVE APPROXIMATION

The procedures are standard. The solution $\underline{\chi}^J(R)$ of Eq. (5) which satisfies standing-wave boundary conditions may be written in the Lippmann-Schwinger integral equation form

$$\underline{\chi}^J=\underline{f}_0^J+G(E)\underline{U}\,\underline{\chi}^J , \tag{8}$$

where $\underline{f}_0^J$ is the regular solution of the free-particle radial Hamiltonian,

$$H_0=-\frac{d^2}{dR^2}+\frac{J(J+1)}{R^2} \tag{9}$$

and $G(E)$ is the principal-value Green's function given by

$$(E-H_0\pm i\epsilon)^{-1}=G(E)\mp i\pi\delta(E-H_0) . \tag{10}$$

In the coordinate representation, Eq. (8) has the form

$$\underline{\chi}^J(R)=\underline{f}_0^J(R)+\int_0^\infty \underline{G}(R,R')\underline{U}(R')\underline{\chi}^J(R')dR' , \tag{11}$$

where the Green's function $\underline{G}(R,R')$ is diagonal. It may be written

$$\underline{G}(R,R')=\underline{k}^{-1}\underline{f}_0^J(R_<)\underline{g}_0^J(R_>) , \tag{12}$$

where $\underline{f}_0^J$ and $\underline{g}_0^J$ are diagonal matrices whose elements are, respectively, regular and irregular Riccati-Bessel or Coulomb functions,[4] depending upon the asymptotic boundary conditions of the scattering channels, and $R_<$ ($R_>$) is the lesser (greater) of $R$ and $R'$. Asymptotically

$$\underline{\chi}^J(R)\sim\underline{f}_0^J(R)-\underline{g}_0^J(R)\underline{k}^{-1/2}\underline{K}\,\underline{k}^{1/2} , \tag{13}$$

where $\underline{K}$ is the reactance matrix,

$$\underline{K}=-\underline{k}^{-1/2}\left[\int_0^\infty \underline{f}_0^J(R)\underline{U}(R)\underline{\chi}^J(R)dR\right]\underline{k}^{-1/2} . \tag{14}$$

The scattering matrix $S$ is given by

$$\underline{S}=(\underline{I}+i\underline{K})(\underline{I}-i\underline{K})^{-1} . \tag{15}$$

If we decompose $\underline{U}$ into the sum of $\underline{U}_1$ and $\underline{U}_2$, Eq. (8) may be replaced by

$$\underline{\chi}_1^J=\underline{f}_1^J+G_1(E)\underline{U}_2\underline{\chi}_1^J , \tag{16}$$

where $\underline{f}_1^J$ is the regular outgoing solution of (11) with $\underline{U}$ replaced by $\underline{U}_1$ and $G_1(E)$ is the principal-value Green's function defined as in Eq. (10) with the Hamiltonian

$$\underline{H}_1=H_0\underline{I}+\underline{U}_1 \tag{17}$$

replacing $H_0$. We choose $\underline{U}_1$ equal to the diagonal part of $\underline{U}$ and $\underline{U}_2$ equal to the off-diagonal part. Then

$$\underline{\chi}_1^J(R)=\underline{f}_1^J(R)+\int_0^\infty \underline{G}_1(R,R')\underline{U}_2(R')\underline{\chi}_1^J(R')dR' . \tag{18}$$

The distorted-wave Green's function is given by

$$\underline{G}_1(R,R')=\underline{k}^{-1}\underline{f}_1^J(R_<)\underline{g}_1^J(R_>) , \tag{19}$$

where $\underline{g}_1^J$ is the irregular outgoing solution of (11) with $\underline{U}$ replaced by $\underline{U}_1$. The solution of Eq. (18) behaves asymptotically as

$$\underline{\chi}_1^J(R)\sim\underline{f}_1^J(R)-\underline{g}_1^J(R)\underline{k}^{-1/2}\underline{K}_1\underline{k}^{1/2} , \tag{20}$$

where

$$\underline{K}_1=-\underline{k}^{-1/2}\left[\int_0^\infty \underline{f}_1^J(R)\underline{U}_2(R)\underline{\chi}_1^J(R)dR\right]\underline{k}^{-1/2} . \tag{21}$$

To relate $\underline{K}_1$ and $\underline{K}$, we introduce the phase shift matrix $\underline{\eta}^J$, whose elements are the elastic scattering phase shifts corresponding to the diagonal potential matrix $\underline{U}_1$. Then, asymptotically,

$$\underline{f}_1^J\sim\underline{f}_0^J\cos\underline{\eta}_J-\underline{g}_0^J\sin\underline{\eta}_J \tag{22}$$

and

$$\underline{g}_1^J\sim\underline{f}_0^J\sin\underline{\eta}_J+\underline{g}_0^J\cos\underline{\eta}_J . \tag{23}$$

Comparing Eqs. (14) and (21), we obtain

$$\underline{K}=(\sin\underline{\eta}_J+\cos\underline{\eta}_J\underline{K}_1)(\cos\underline{\eta}_J-\sin\underline{\eta}_J\underline{K}_1)^{-1} . \tag{24}$$

If $\underline{U}_2(R)$ is small, Eqs. (20) and (21) for $\underline{K}_1$ may be usefully solved by an iterative process. To first order in $\underline{U}_2$,

$$\underline{K}_1^{(1)} = -\underline{k}^{-1/2} \left[ \int_0^\infty \underline{f}_1^J(R)\underline{U}_2(R)\underline{f}_1^J(R)dR \right] \underline{k}^{-1/2} . \quad (25)$$

Expression (25) is the first-order distorted-wave approximation. Because it is a symmetric matrix the resulting $S$ matrix is unitary.

Iterating again we obtain a second-order distorted-wave approximation

$$\underline{K}_1^{(2)} = -\underline{k}^{-1/2} \left[ \int_0^\infty dR\, \underline{f}_1^J(R)\underline{U}_2(R) \int_0^\infty dR'\underline{G}_1(R,R')\underline{U}_2(R')\underline{f}_1^J(R') \right] \underline{k}^{-1/2} . \quad (26)$$

The first-order reactance matrix $\underline{K}_1^{(1)}$ is symmetric, but the matrix $\underline{K}_1^{(2)}$ may not be. To enforce symmetry and obtain a unitary $S$ matrix to second order in $\underline{U}_2$ we calculated the matrix element $\underline{K}_1^{(2)}(ij)$ for any pair of scattering channels with $i \geq j$ and took $\underline{K}_1^{(2)}(ij) = \underline{K}_1^{(2)}(ji)$ for $i < j$.

## IV. RESULTS

The accuracy of the distorted-wave approximations was tested by comparison with full close-coupled results for the charge transfer process[5]

$$C^{3+} + H \rightarrow C^{2+} + H^+ . \quad (27)$$

The diagonal diabatic potential-energy curves $\underline{U}_1(R)$ for three scattering channels of $^1\Sigma^+$ molecular symmetry are reproduced in Fig. 1 and the diabatic coupling matrix elements $U_2$ in Fig. 2. Channel 3 is the entrance channel separating to $C^{3+}$ and H, channel 2 is the exit channel separating to $C^{2+}(2p^2\,{}^1S)$ and $H^+$, and channel 1 is the exit channel separating to $C^{2+}(2p^2\,{}^1D)$ and $H^+$.

We reduced $\underline{U}_2$ by multiplication by a factor $\lambda$ equal successively to $10^{-3}$, $10^{-2}$, $10^{-1}$, and unity. The close-coupled solutions were obtained by the log-derivative method of Johnson.[6] The distorted-wave solutions were obtained using Numerov integration[7] and the quadratures were carried out with Simpson's composite formula.[8] The two procedures have overall errors of order $h^4$ where $h$ is the interval size and are well matched.

Calculations were carried out at an energy $E$ of 10 eV/amu in the entrance channel. For $\lambda = 10^{-3}$ and $10^{-2}$, the first-order distorted-wave approximation to the squared modulus of the off-diagonal matrix elements $|S_{ij}|^2$ of the scattering matrix defined in Eq. (15) was identical for all $J$ to the exact values. For $\lambda = 10^{-1}$, differences occurred between the first-order distorted wave and exact values which became serious for $J < 60$. Figure 3 illustrates the values of $|S_{12}|^2$ as a function of $J$. The second-order distorted-wave approximation is a substantial improvement over the first-order approximation and agrees closely with the close-coupled results for $J$ greater than about 15. The behavior of $|S_{13}|^2$ and $|S_{23}|^2$ is similar.

For the actual coupling case $\lambda = 1$, the first- and second-order distorted-wave approximations fail completely and it is probable that the distorted-wave series does not converge except at uninterestingly large values of $J$. However, the distorted-wave methods become more accurate with increasing energy as $\lambda \underline{U}_2/E$ decreases. Figure 4 presents the results for $\lambda = 1$ at an incident energy of 1 keV/amu. The first-order distorted-wave approximation is adequate for $J$ greater than 1400. The second-order approximation tracks the exact values well down to $J$ equal to 400, sometimes overestimating and sometimes underestimating $|S_{23}|^2$. To obtain a reliable cross section, close-coupled solutions are required only for $J < 400$.

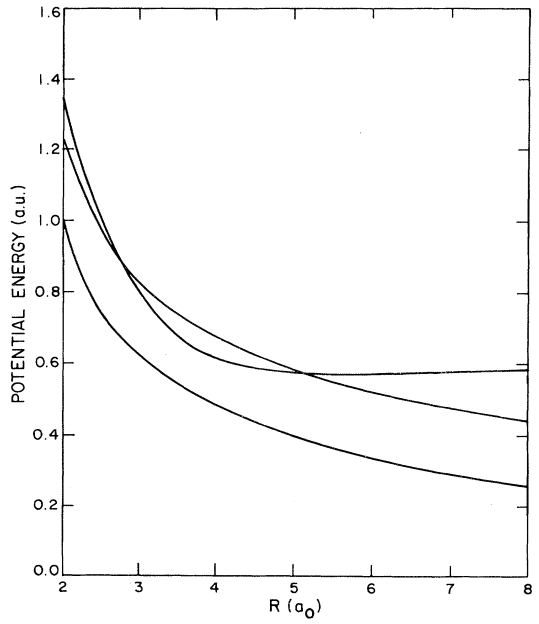


FIG. 1. $CH^{3+}$ diabatic potential-energy curves of $^1\Sigma^+$ symmetry. Dissociation limits are, with increasing energy, $C^{2+}(2p^2\,{}^1D) + H^+$, $C^{2+}(2p^2\,{}^1S) + H^+$, and ground state $C^{3+} + H$.

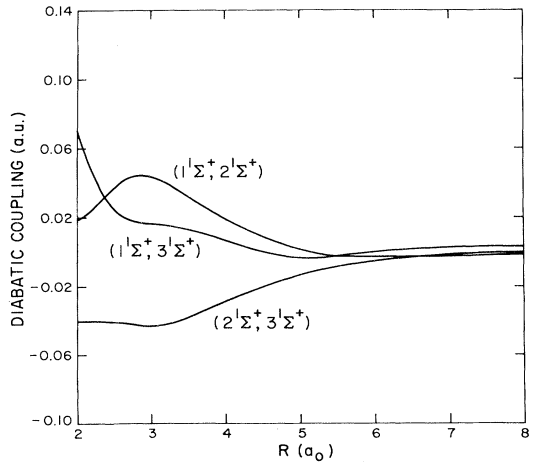


FIG. 2. $CH^{3+}$ diabatic coupling matrix elements between the states given in Fig. 1.

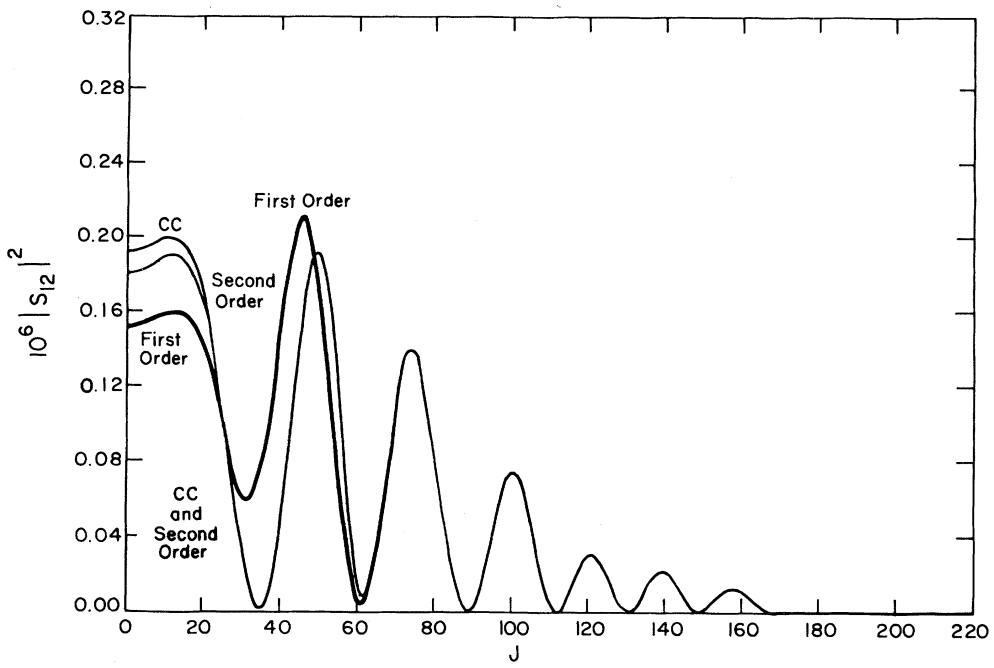


FIG. 3. $|S_{12}|^2$ as a function of partial-wave quantum number $J$ at $E=10$ eV/amu using close-coupling (CC) and first- and second-order distorted-wave approximations with a coupling strength of $\lambda=0.1$.

In practice, we use close-coupled results at low $J$ which give way to the second-order distorted-wave approximation and then to the first-order distorted-wave approximation as each becomes sufficiently accurate. The procedure permits the calculation of heavy-particle collision cross sections at energies up to 10 kev/amu. Further economies are possible and extension to higher energies could be achieved by the use of the Jeffreys-Wentzel-Kramers-

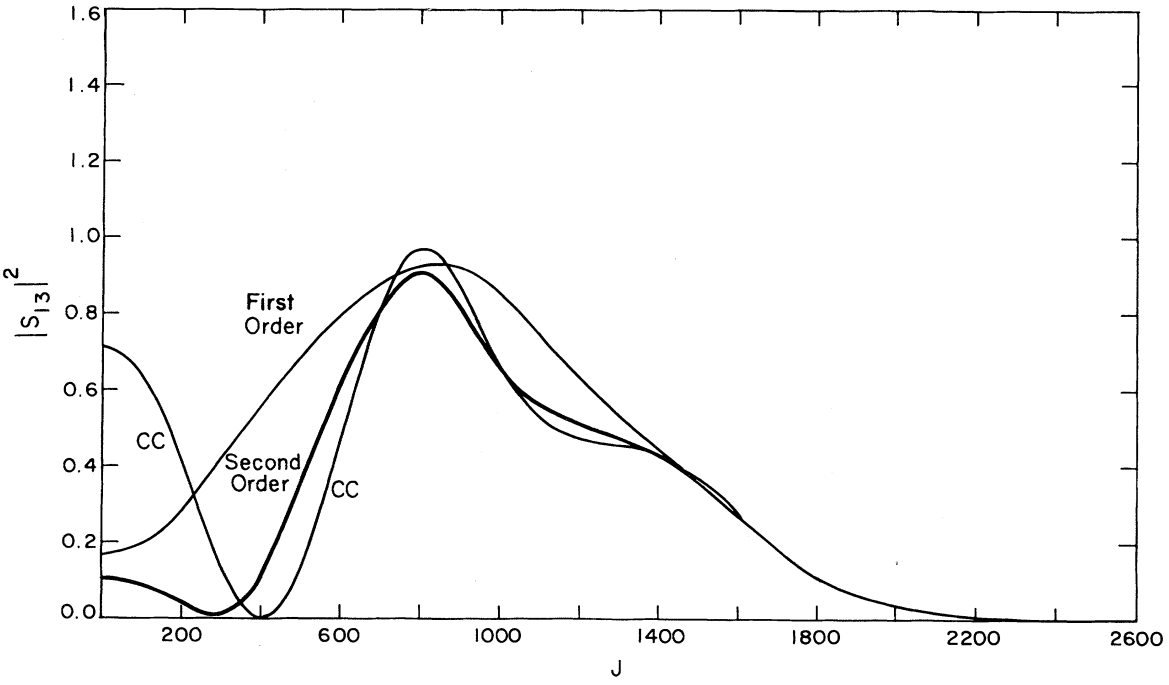


FIG. 4. Close-coupled (CC) and first- and second-order distorted-wave values of $|S_{13}|^2$ vs $J$ at $E=1$ keV/amu and a coupling strength $\lambda=1.0$.

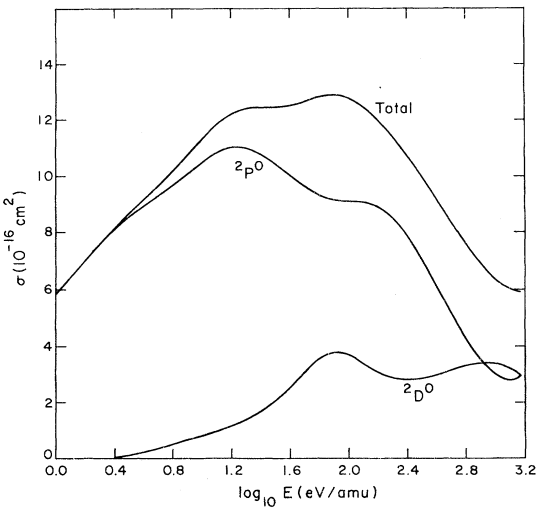


FIG. 5. Total charge transfer cross section and individual sections for the population of metastable $^2P^o$ and $^2D^o$ levels of $O^+$ in the reaction $O^{2+} + He \rightarrow O^+ + He^+$.

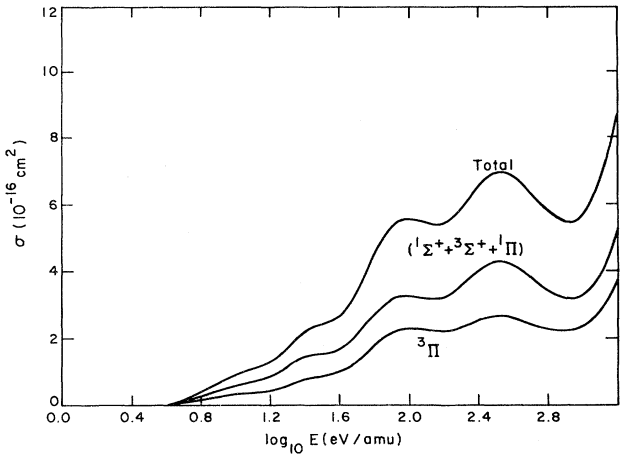


FIG. 6. Cross sections for the transition $O^+(^2D^o) \rightarrow O^+(^2P^o)$ induced by $He^+$ impact. The curve labeled $^3\Pi$ is the result for the $^3\Pi$ channel which interacts with the charge transfer channel. The curve labeled ($^1\Sigma^+ + ^3\Sigma^+ + ^1\Pi$) is an estimate of the contributions from the other molecular symmetries. The sum over all channels is shown by the curve labeled "Total."

Brillouin (JWKB) approximation to the functions $\underline{f}^J_1(R)$ and $\underline{g}^J_1(R)$.

## V. CHARGE TRANSFER OF $O^{2+}$ IN He

Charge transfer cross sections of $O^{2+}$ ions in helium have been calculated at thermal energies.[9] Three $^3\Pi$ molecular states appear to be significant. The diabatic potential-energy curves and coupling elements have been reported by Butler *et al.*[10] We use them here in conjunction with the distorted-wave approximation to extend the calculations to energies of 5 keV. Throughout most of the energy range, charge transfer preferentially populates the $O^+(2p^3\,^2P^o)$ state but near 5 keV capture into the $O^+(2p^3\,^2D^o)$ state becomes of comparable importance. The calculated cross sections are shown in Fig. 5. The total charge transfer rate coefficient has been measured at 400 K (Ref. 11) to be $(3.5\pm1.5)\times10^{-11}$ cm$^3$ s$^{-1}$ in agreement with the theoretical value of $2\times10^{-11}$ cm$^3$ s$^{-1}$ but there are no data at higher energies.

TABLE I. Cross sections in units of $10^{-16}$ cm$^2$ for the process $He^+ + O^+(^2D^o) \rightarrow He^+ + O^+(^2P^o)$ in the $^3\Pi$ channel of $OHe^{2+}$ as a function of the energy $E$ in eV of relative motion in the initial channel. [We use the notation $4.4(-7) \equiv 4.4\times10^{-7}$.]

| $E$ (eV) | Two state | Three state |
|---|---|---|
| 7.35 | 4.4(−7) | 5.3(−7) |
| 8.16 | 6.6(−5) | 5.6(−5) |
| 13.6 | 3.5(−2) | 2.4(−2) |
| 32.2 | 1.11 | 0.642 |
| 57.2 | 1.94 | 0.984 |
| 82.2 | 2.87 | 1.59 |
| 132.2 | 3.38 | 2.06 |
| 257.2 | 6.32 | 4.34 |
| 507.2 | 6.41 | 4.40 |
| 1007.2 | 8.51 | 5.34 |
| 2007.2 | 6.91 | 4.60 |
| 5007.2 | 10.3 | 7.34 |

Cross sections for transitions between the metastable $O^+(^2P^o)$ and $O^+(^2D^o)$ states induced by the impact of $He^+$ ions in the $^3\Pi$ molecular symmetry can also be calculated with our procedures. The transition may occur by a direct impact excitation through the quadrupole component of the interaction,[12] and indirectly by crossings into and out of the charge transfer channel. We present in Table I the cross sections for the process (3) calculated in the two-state approximation which ignores the charge transfer channel and in the three-state approximation which includes it. Except at very low impact energies, the inclusion of the charge transfer channel extracts flux from the direct excitation channel and diminishes the excitation cross sections. Below 8 eV, the additional path for excitation provided by crossings into and out of the charge transfer state augments the excitation cross section.

The process (3) also takes place in the $^1\Sigma$, $^3\Sigma$, and $^1\Pi$ molecular symmetry states. For them, the potential-energy curves and coupling matrix elements are not available. However, unlike the $^3\Pi$ states they do not undergo avoided crossings with any charge transfer state and at low energies the transition is driven by the interaction between the $He^+$ ion and the quadrupole moment of the target. Thus the cross sections are not much different from those obtained for the $^3\Pi$ state in the two-state approximation when charge transfer is ignored. Our estimates for the total cross section, summed over all channels, for the excitation of $O^+(^2D^o)$ to $O^+(^2P^o)$ by helium-ion impact are presented in Fig. 6 as a function of energy. For temperatures in excess of about $10^6$ K, helium-ion impacts are more effective than electron impacts[13] in exciting the $^2D^o$-$^2P^o$ metastable transition.

## ACKNOWLEDGMENT

This work was supported in part by the Division of Chemical Sciences of the U.S. Department of Energy.

[1]T. G. Heil, S. E. Butler, and A. Dalgarno, Phys. Rev. A 23, 1100 (1981).
[2]J. B. Delos and W. R. Thorson, Phys. Rev. A 18, 117 (1978); 18, 135 (1978); J. Chem. Phys. 70, 1774 (1979).
[3]H. Ryufuku and T. Watanabe, Phys. Rev. A 18, 2005 (1978); 19, 1538 (1979).
[4]*Handbook of Mathematical Functions,* U.S. Natl. Bur. Stand. (Appl. Math. Ser. No. 55), edited by M. Abramowitz and I. A. Stegun (U.S. GPO, Washington, D.C., 1970).
[5]S. Bienstock, T. G. Heil, C. Bottcher, and A. Dalgarno, Phys. Rev. A 25, 2850 (1982).
[6]B. R. Johnson, J. Comput. Phys. 13, 445 (1973).
[7]A. C. Allison, Comput. Phys. Commun. 1, 21 (1969).
[8]D. M. Young and R. T. Gregory, *A Survey of Numerical Mathematics* (Addison-Wesley, Reading, Mass., 1972), Vol. 1.
[9]A. Dalgarno, S. E. Butler, and T. G. Heil, J. Geophys. Res. 85, 6047 (1980).
[10]S. E. Butler, T. G. Heil, and A. Dalgarno, J. Chem. Phys. (to be published).
[11]R. Johnsen and M. A. Biondi, J. Chem. Phys. 74, 305 (1981).
[12]D. A. Landman, Sol. Phys. 30, 371 (1973); 31, 81 (1973); Astrophys. J. 220, 366 (1978).
[13]R. J. W. Henry, Phys. Rep. 68, 1 (1981).